

Increased Ras Expression and Caspase-Independent Neuroblastoma Cell Death: Possible Mechanism of Spontaneous Neuroblastoma Regression

Chifumi Kitanaka, Keisuke Kato, Rieko Ijiri, Kaori Sakurada, Arata Tomiyama, Kohji Noguchi, Yohji Nagashima, Akira Nakagawara, Takashi Momoi, Yasunori Toyoda, Hisato Kigasawa, Toshiji Nishi, Mikako Shirouzu, Shigeyuki Yokoyama, Yukichi Tanaka, Yoshiyuki Kuchino

Background: Neuroblastoma undergoes spontaneous regression frequently during its natural course. Although programmed cell death (PCD) has been implicated in this process, accumulating evidence suggests that apoptosis, a form of PCD that is regulated by caspases, may not play a major role. We examined the mechanism(s) of spontaneous regression of neuroblastoma, focusing on the role of Ras, a favorable prognostic marker of neuroblastoma. **Methods:** Tumor tissues were analyzed by light microscopy, electron microscopy, and immunohistochemistry to examine cell degeneration and expression of Ras and several indicators of PCD. Cell degeneration was also studied *in vitro* in neuroblastoma cells transfected with the H-ras gene. All statistical tests were two-sided. **Results:** Immunohistochemical analyses revealed that Ras expression was increased in areas of cellular degeneration lacking apoptotic characteristics. The degenerating cells were fragmented without nuclear condensation and, essentially, lacked caspase-3 activation and apoptotic DNA fragmentation. These cells had ultrastructural features of autophagic degeneration, another form of PCD that is distinct from apoptosis. Focal areas of degeneration associated with Ras expression were seen more frequently in tumors from patients detected in a mass-screening program (53 [60.9%] of 87) than in tumors from clinically detected, advanced-stage patients over 1 year of age (7 [29.2%] of 24) ($P = .006$; chi-square test), suggesting a positive relationship between Ras-associated degeneration and probability of spontaneous regression/favorable prognosis. The characteristic features of Ras-associated nonapoptotic degeneration observed in tumor samples were recapitulated *in vitro* by transfection-mediated Ras expression, and Ras-mediated degeneration was augmented by TrkA, another favorable prognostic marker. **Conclusions:** High-level expression of H-Ras in neuroblastoma cells is associated with caspase cascade-independent, nonapoptotic PCD. This Ras-mediated nonapoptotic tumor cell death may play a key role in spontaneous regression of neuroblastoma. [J Natl Cancer Inst 2002;94:358–68]

Spontaneous regression (resolution) of cancer is a rare event of outstanding biological interest and significance. Nevertheless, the underlying mechanism is only poorly understood. Neuroblastoma is a common childhood malignancy in which spontaneous regression is by far the most frequently observed among

a variety of cancers (1,2), and it therefore has been an attractive target of research to elucidate the mechanism. Accumulating evidence suggested that spontaneous regression of neuroblastoma most likely occurs by the programmed death of tumor cells rather than by spontaneous maturation (differentiation) alone or by immunological attack on tumor cells (1). This led to the assumption that apoptosis, a representative form of programmed cell death (PCD), may play an important role in the spontaneous regression of neuroblastoma. However, despite substantial efforts to identify a critical role for apoptosis in the process of regression, the results were inconclusive. Although some groups found somewhat increased incidence of terminal deoxynucleotidyl transferase-mediated deoxyuridine triphosphate (dUTP) nick-end labeling (TUNEL)-positive cells in neuroblastomas with a higher probability of spontaneous regression (3,4), others failed to find evidence of a correlation between apoptosis and factors associated with spontaneous regression (5–7). In support of this, recent electron microscopic analysis revealed that degenerative changes are a conspicuous feature of neuroblastoma and that these changes are characterized by accumulation of myelinated bodies, dense or lamellated lysosomes, and autophagic vacuoles (8). These observations suggest that spontaneous neuroblastoma cell death may occur via autophagic degeneration, another form of PCD distinct from apoptosis (9).

On the other hand, molecular biologic markers such as H-Ras, TrkA, and N-Myc have been associated with the prognosis

Affiliations of authors: C. Kitanaka, K. Sakurada, A. Tomiyama, K. Noguchi, Y. Kuchino, Biophysics Division, National Cancer Center Research Institute, Chuo-ku, Tokyo, Japan; K. Kato, R. Ijiri, Y. Tanaka (Division of Pathology), Y. Toyoda (Division of Oncology), H. Kigasawa (Division of Hematology), T. Nishi (Division of Surgery), Kanagawa Children's Medical Center, Minami-ku, Yokohama, Japan; Y. Nagashima, Second Department of Pathology, School of Medicine, Yokohama City University, Kanazawa-ku, Yokohama; A. Nakagawara, Division of Biochemistry, Chiba Cancer Center Research Institute, Chuoh-ku, Chiba, Japan; T. Momoi, Division of Development and Differentiation, National Institute of Neuroscience, National Center of Neurology and Psychiatry, Kodaira, Tokyo; M. Shirouzu, S. Yokoyama, Genomic Sciences Center, RIKEN Yokohama Institute, Tsurumi, Yokohama; S. Yokoyama, Department of Biophysics and Biochemistry, Graduate School of Science, University of Tokyo, Bunkyo-ku, Tokyo; Y. Kuchino, Core Research for Evolutional Science and Technology, Japan Science and Technology Corporation, Kawaguchi, Saitama, Japan.

Correspondence to: C. Kitanaka, M.D., or Y. Kuchino, Ph.D., Biophysics Division, National Cancer Center Research Institute, 5-1-1 Tsukiji, Chuo-ku, Tokyo 104-0045, Japan (e-mail: ckitanak@ncc.go.jp).

See "Note" following "References."

© Oxford University Press

of neuroblastoma. The amplification and/or overexpression of the N-myc gene have been associated with poor prognosis (10). In contrast, the overexpression of H-Ras as well as TrkA is a favorable prognostic factor of neuroblastoma (11–15), suggesting that H-Ras and/or TrkA overexpression might contribute to the elimination of tumor cells through an as yet unknown mechanism. Given our recent observation (9,16) that Ras causes autophagic degeneration in a cell type-dependent manner, these lines of evidence together give rise to the intriguing possibility that increased expression of Ras may contribute to neuroblastoma regression through the activation of a nonapoptotic cell suicide program. In this study, we examine this possibility—through *in vivo* analyses using neuroblastoma tissues and through *in vitro* analyses using neuroblastoma cell lines—for the purpose of understanding the mechanism involved in spontaneous neuroblastoma regression.

MATERIALS AND METHODS

Analyses of Tumor Samples from Neuroblastoma Patients

Tumor samples were obtained from neuroblastoma patients identified through the mass screening program (2,17) (mass screened patients) and, for comparison, from patients (≥ 1 year old) clinically detected and at stage 3 or 4 according to the International Neuroblastoma Staging System (INSS) (18) (clinically detected, advanced-stage patients over 1 year of age), who underwent tumor resection at Kanagawa Children's Medical Center from 1972 through 1999. Tumor samples obtained from patients who received preoperative chemotherapy or radiotherapy and those tumors less than 1 cm in diameter or judged to be not suitable for immunohistochemistry because of poor sample preparation (this was checked by a pilot immunohistochemical analysis using antibodies such as anti-neurofilament and anti-CD68) were excluded. As a result, a total of 87 tumors from mass screened patients and 24 tumors from clinically detected, advanced-stage patients over 1 year of age were available for the following analyses in this study.

For immunohistochemical analyses, sections from formalin-fixed, paraffin-embedded tumor samples were used. After xylene deparaffinization and ethanol rehydration, the samples were treated with 0.3% hydrogen peroxide in methanol to inactivate endogenous peroxidase and then subjected to microwave treatment in 0.01 M citrate buffer (pH 6.0) for antigen retrieval. To detect the H-Ras protein, the tissue sections were first treated with 5% normal swine serum to block nonspecific staining, followed by incubation first with anti-c-H-Ras mouse monoclonal antibody (Ab-1, 1:100 dilution; Calbiochem, San Diego, CA) overnight at 4°C and then with a peroxidase-conjugated anti-mouse immunoglobulin G rat antibody (1:50 dilution) for 1 hour at room temperature (MBL, Nagoya, Japan). Bound antibody was visualized using diaminobenzidine as a chromogen, and the sections were lightly counterstained with hematoxylin. The specificity of H-Ras immunostaining was confirmed by omission of the primary antibody and the use of multiple irrelevant primary antibodies and by the immunoadsorption method (preincubation of the anti-c-H-Ras antibody with recombinant human c-H-Ras protein fused to glutathione S-transferase [Calbiochem]). Parenchymatous cells of the adrenal gland and connective tissues served as positive and negative controls, respectively, in H-Ras immunostaining of tumor samples (19). For evaluation of Ras immunoreactivity, a simple two-staged grad-

ing was adopted; i.e., positive or negative. Only cells unequivocally positive for Ras were judged to be Ras positive, and the others were judged to be Ras negative. A focal area of degeneration associated with Ras expression was defined as a cluster (20 or more cells or cell fragments) of Ras-positive, degenerating tumor cells without intervening Ras-negative, nondegenerating tumor cells. For the semiquantitative assessment of the appearance of focal areas of degeneration associated with Ras expression for each tumor, we examined one set of tumor sections stained with hematoxylin–eosin (H&E) and their adjacent sections stained with the anti-Ras antibody; a tumor sample was judged to be negative if the set analyzed contained no focal areas of degeneration associated with Ras expression and to be positive if the set contained one or more such focal areas. Immunostaining with antibody against active caspase-3 fragments (p20/p17) and TUNEL analysis of paraffin sections have been described (20,21).

For electron microscopy, tumor samples were fixed with 2.5% glutaraldehyde, postfixed with 2% OsO₄, and embedded in Epon. Semithin sections (1 μ m) were stained by the periodic acid-Schiff (PAS) method (oxidation in 1% aqueous periodic acid for 10 min, followed by treating for 10 min with Schiff's reagent and rinsing in a sulfurous acid solution). After localization of PAS-positive, degenerating cells in semithin sections, the contiguous tumor samples were trimmed under a microscope, and serial adjacent ultrathin sections (~ 0.04 μ m) encompassing PAS-positive, degenerating cells were cut. The ultrathin sections were then examined by transmission electron microscopy after staining with uranyl acetate and lead citrate.

Plasmids and Reagents

pcDNA3wtRas and pcDNA3RasV12 express wild-type and constitutively activated oncogenic H-Ras proteins, respectively, under the control of the cytomegalovirus immediate early promoter of the pcDNA3 expression vector (Invitrogen, Groningen, The Netherlands). cDNAs coding for enhanced green fluorescent protein (GFP), baculovirus p35 protein, and mouse Bcl-xL was subcloned into pcDNA3 to create pcDNA3EGFP, pcDNA3p35, and pcDNA3mbclxL, respectively. The entire coding region of human TrkA cDNA was subcloned into pFLAG CMV2 (Kodak, New Haven, CT) in-frame to the FLAG epitope to create pTrkA. Plasmids for inducible expression, pTA-Hyg, pT2-GN, pT2-wtRas, and pT2-RasV12, have been described (16). Staurosporine was purchased from Sigma Chemical Co. (St. Louis, MO). zVAD-fmk and zAsp-CH₂-DCB were obtained from Peptide Institute (Osaka, Japan). Boc-Asp-fmk and β -nerve growth factor (NGF) were purchased from Calbiochem.

Cells, Transfection, and Colony Formation Assay

Human neuroblastoma cell lines SH-SY5Y and GAMB were maintained on collagen I-coated dishes (Biocoat; BD Biosciences, Franklin Lakes, NJ) in RPMI 1640 medium (Sigma) supplemented with 10% fetal bovine serum (Multiser; Cytosystems, Castle Hill, Australia). For transfection, neuroblastoma cells (2×10^5) were seeded into 60-mm dishes 2 days before transfection, and transfection was done using Effectene transfection reagent (Qiagen, Hilden, Germany) according to the manufacturer's instruction. The total amount of transfected DNA was always kept constant by use of an empty vector plasmid. Colony formation assay was done essentially as described (16). In brief, neuroblastoma cells transfected with 1 μ g of

pcDNA3-based expression plasmids were cultured in the presence of a selection drug (800 $\mu\text{g}/\text{mL}$ Geneticin (GIBCO BRL, Rockville, MD) for approximately 2 weeks, and the number of colonies formed after drug selection was counted under a phase contrast microscope.

Immunoblot Analyses

Both adherent and detached cells were collected and were subjected to lysis in the lysis buffer (25 mM Tris-HCl pH 7.6, 50 mM NaCl, 2% Nonidet P-40, 0.5% deoxycholate, 0.2% sodium dodecyl sulfate). After determination of protein concentrations, equal amounts of cell lysates were separated by SDS-polyacrylamide gel electrophoresis (15% for Ras and 8% for poly[ADP-ribose] polymerase [PARP]), transferred to a nitrocellulose membrane, and blotted first with a primary antibody against c-H-Ras (Ab-1; Calbiochem, or C-20; Santa Cruz Biotechnology, Santa Cruz, CA) or PARP (rabbit polyclonal; Boehringer Mannheim, Mannheim, Germany) and subsequently with an appropriate horseradish peroxidase-conjugated secondary antibody (Zymed, South San Francisco, CA). Blots were visualized by enhanced chemiluminescence (ECL; Amersham-Pharmacia, Buckinghamshire, England).

Generation and Analyses of Cell Lines Inducible with Tetracycline Withdrawal

SH-SY5Y-TA-GN, SH-SY5Y-TA-wtRas, and SH-SY5Y-TA-RasV12 cells were established by cotransfection of SH-SY5Y cells with pT2-GN, pT2-wtRas, and pT2-RasV12, respectively, together with pTA-Hyg followed by drug selection with Hygromycin B (Calbiochem) and Geneticin (GIBCO BRL). Inducible expression of LacZ (in SH-SY5Y-TA-GN cells), wt-Ras, and RasV12 was verified by immunoblot analyses. The stable transfectants were maintained in the presence of 400 U/mL Hygromycin B, 200 $\mu\text{g}/\text{mL}$ Geneticin, and 0.5 $\mu\text{g}/\text{mL}$ tetracycline (Sigma). The percentage of cell death was defined as $100 \times (\text{number of dead cells})/(\text{number of dead cells} + \text{number of live cells})$. Dead cells were detected by their loss of ability to exclude trypan blue dye, but small fragments of dead cells with a diameter apparently shorter than half that of live cells were not counted. Transmission electron microscopic analysis was carried out as described (16). TUNEL assay was done using an *in situ* apoptosis detection kit (Wako, Osaka, Japan) according to the manufacturer's instructions. In brief, cells seeded on a collagen I-coated glass coverslip and treated as described in the figure legends were fixed in phosphate-buffered saline with 4% formaldehyde. After treatment with the permeabilization buffer (0.1% sodium citrate-0.1% Triton X-100), cells were incubated first with terminal deoxynucleotidyl transferase and fluorescein isothiocyanate (FITC)-labeled dUTP and then with peroxidase-conjugated anti-FITC antibody. A positive signal was visualized by the addition of diaminobenzidine. For propidium iodide staining, cells were instead incubated with a 25 $\mu\text{g}/\text{mL}$ propidium iodide (Sigma) solution after the permeabilization step. Analyses of inducible cell lines were done using multiple independent clones for each cell line, and essentially identical results were obtained from different clones of each. The results of representative clones are presented.

Statistical Analysis

The chi-square test was used to determine distribution differences in the frequency of the appearance of focal areas of de-

generation associated with Ras expression between tumors from mass screened patients and from clinically detected, advanced-stage patients over 1 year of age; a *P* value of less than .05 was considered to be statistically significant. The results of quantitative *in vitro* analyses were presented as the mean and 95% confidence intervals. All statistical analyses were two-sided.

RESULTS

Ras Expression and Autophagic Tumor Cell Degeneration in Neuroblastoma Tissues

To test the idea that Ras expression mediates neuroblastoma cell death, we first examined the morphology of neuroblastoma cells expressing Ras protein using tumor samples from neuroblastoma patients. It has been well documented that H-Ras protein is expressed at high levels in neuroblastomas with a favorable prognosis—including those detected through mass screening (11,12,14,22). Consistent with such reports, pilot immunohistochemical analysis of mass screened tumors detected definite H-Ras immunoreactivity in these tumors. We then went on, using serial tumor sections, to compare corresponding areas stained with anti-H-Ras antibody and with H&E. Strikingly, we found that intense H-Ras staining clearly colocalizes with cells that are undergoing or have undergone degeneration in H&E sections (Fig. 1, compare A-a with A-b, B-a with B-b, C-a with C-b, and D-a with D-b). Closer analysis at a higher magnification revealed that the degenerating nuclei do not show apparent chromatin condensation and undergo extensive fragmentation (Fig. 1, D-e; the double arrows indicate fragmented nuclei, whereas the single arrows indicate unfragmented ones). Fragmentation of the degenerating cells was also evident from the marked irregularity in size of cellular debris and of immunoreactive signals for Ras (Fig. 1, A-b, B-b, C-b, D-b, and E). Such Ras-positive, degenerating cells were found either scattered among viable cells (Fig. 1, E) or as focal areas of cellular degeneration (Fig. 1, A-D) and either distant from or close to fibrovascular stroma. Similar findings were observed also in tumors from clinically detected, advanced-stage patients over 1 year of age known to have a poor prognosis (10). However, consistent with previous observations that H-Ras overexpression occurs more frequently in neuroblastomas with a favorable prognosis (11,12,14,22), focal areas of degeneration associated with H-Ras expression were found statistically significantly more frequently in tumors from mass screened patients than in those from clinically detected, advanced-stage patients over 1 year of age (53 of 87 versus 7 of 24, respectively; *P* = .006) (Table 1).

As the morphology of degenerating tumor cells positive for Ras was apparently distinct from that of apoptosis characterized by definite nuclear condensation, we examined the tumor sections for the evidence of activation of caspase cascade and apoptotic DNA fragmentation with 3'-OH ends by active caspase-3 and TUNEL staining, respectively. The results indicated that Ras-positive degenerating cells were essentially negative for caspase-3 activation as well as for apoptotic DNA fragmentation (Fig. 1, compare C-b with C-c or C-d, and D-b with D-c), providing biochemical evidence that tumor cells overexpressing Ras are undergoing a caspase-independent, nonapoptotic cell death. We then asked whether autophagic degeneration, a nonapoptotic type of PCD that can be induced by Ras overexpression (9,16), is involved in the cell death process. It has recently been shown that autophagic vacuoles (lysosomes) stain positive

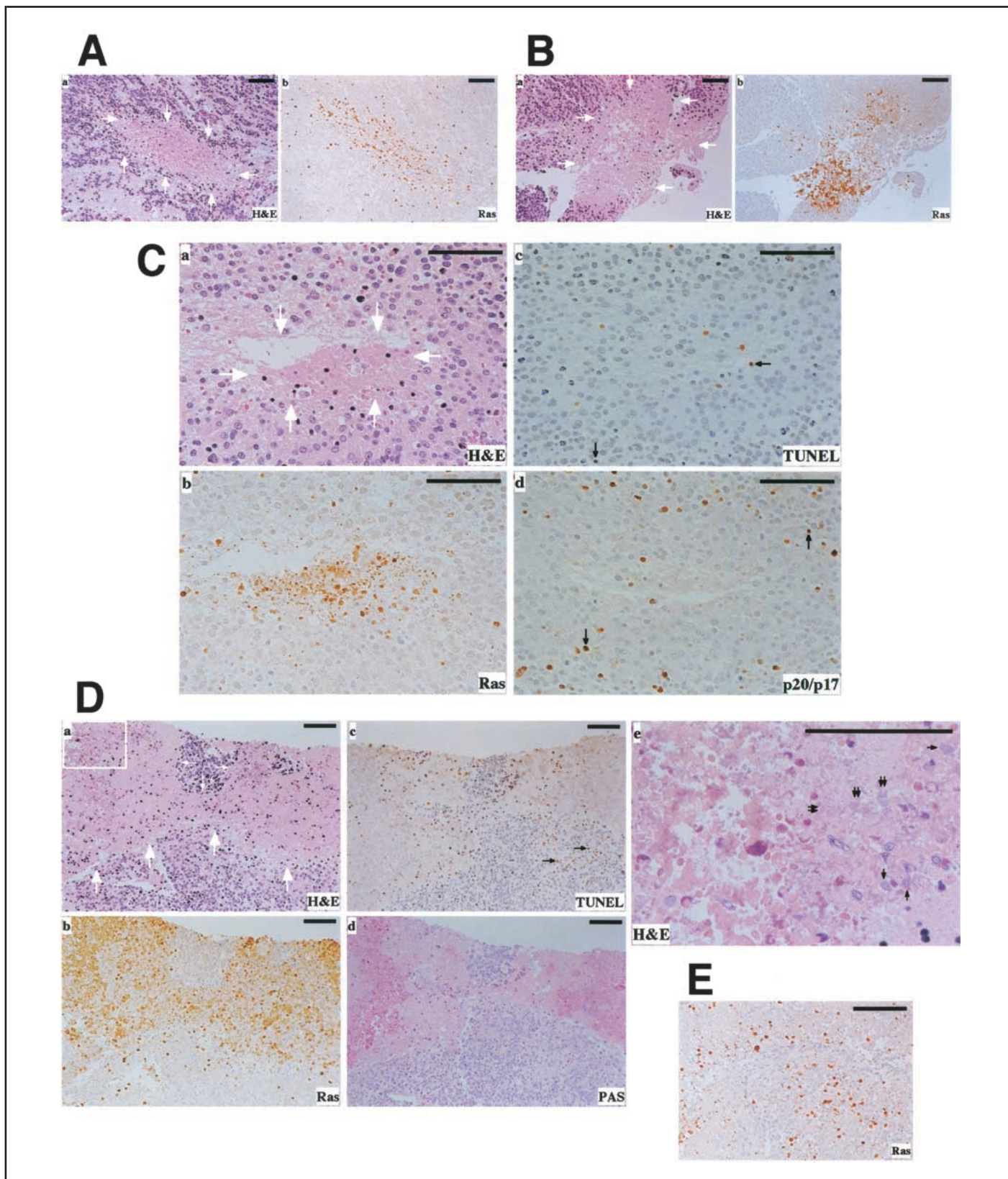


Fig. 1. Ras overexpression and nonapoptotic degeneration of tumor cells in neuroblastoma tissues. Serial tumor sections (A-a, b), (B-a, b), (C-a, b, c, d), and (D-a, b, c, d) were stained either with anti-H-Ras (Ras), with anti-p20/p17 active caspase-3 fragments (p20/p17), with hematoxylin-eosin (H&E), by the terminal deoxynucleotidyl transferase-mediated deoxyuridine triphosphate nick-end labeling (TUNEL) method, or by the periodic acid-Schiff (PAS) method, as indicated in each panel. A single section was stained with anti-H-Ras antibody and shown in panel (E). Positive signals for immunostaining and TUNEL assay appear brown, and positive PAS staining appears red-purple. In the H&E-stained

sections of (A) through (D), the margins of degenerating areas are marked by **white arrows**. In (C), the presence of a gap within the degenerating area may reflect active retraction (shrinkage) of the tissue following degeneration. In (C) and (D), samples of typical apoptotic cells with positive staining for active caspase-3 (C-d) or TUNEL (C-c and D-c) are indicated by **black arrows**. (D-e) is a magnified view of the boxed area in (D-a). Samples of unfragmented degenerating nuclei and clusters of fragmented nuclei are indicated by **single** and **double arrows**, respectively, in (D-e). Scale bars = 100 μ m.

Table 1. Relationship of Ras-associated degeneration with patient and tumor characteristics*

	INSS stage	Areas of degeneration associated with Ras expression		P
		Negative	Positive (%)	
Mass screened NB	1	21	27	
	2	9	18	
	3	4	7	
	4	0	1	
	4s	0	0	
Total		34	53 (60.9)	
Clinically detected, advanced-stage NB (≥ 1 y)	3	1	0	
	4	16	7	
Total		17	7 (29.2)	.006†

*NB = neuroblastoma; INSS = International Neuroblastoma Staging System.

†Comparison was made of the proportions of positive cases between mass screened NB and clinically detected, advanced-stage NB (≥ 1 y), and the difference was tested (two-sided) by the chi-square test.

for PAS (23), and positive PAS staining has been indeed demonstrated in neurodegenerative diseases in which autophagic degeneration has been implicated (9,24). PAS staining of serial adjacent sections revealed that Ras-positive degenerating cells are often positive for PAS (Fig. 1, D-d). Taking advantage of this association of PAS and Ras staining, we could analyze the ultrastructure of the degenerating cells under fixation conditions in which fine structures are highly preserved (see "Materials and Methods"). Electron microscopic analysis of degenerating cells presumed to be positive for PAS, and hence for Ras as well, showed a definite increase of primary lysosomes and autolysosomes in the cytoplasm and lack of nuclear condensation when compared with nondegenerating tumor cells (Fig. 2, B); these are characteristic features of autophagic degeneration (Fig. 2, A). In addition, the presence of cellular fragments containing lysosomal structures (Fig. 2, double arrows in both panels) suggests that degenerating cells undergo fragmentation after autophagic changes.

Induction of Neuroblastoma Cell Death by Ras Expression *In Vitro*

The above *in vivo* observations using tumor samples from neuroblastoma patients clearly indicated that Ras overexpression in human neuroblastoma is closely associated with caspase-independent, nonapoptotic tumor cell death. We then examined *in vitro*—using human neuroblastoma cell lines—whether Ras expression is the cause of such cell death. In human neuroblastoma, ras gene mutations frequently found in other human cancers are quite rare, suggesting that mutational activation of Ras does not have a role in the genesis and development of human neuroblastoma (25,26). Nevertheless, a constitutively activated H-Ras with oncogenic mutation (RasV12) was used in this study in addition to wild-type H-Ras (wt-Ras) for the purpose of efficient activation of the Ras signaling pathway. We tested a series of human neuroblastoma cell lines (SH-SY5Y, GAMB, IMR32, LA-N-5, SMS-KCN, TGW, and RTBM-1) to examine the effect of wt-Ras and RasV12 expression. Of these neuroblastoma cell lines, we could achieve Ras expression levels comparable to those expressed in tumor samples on immunoblot analysis in SH-SY5Y and GAMB cells (data not shown), and therefore subjected these cell lines to subsequent analyses. As

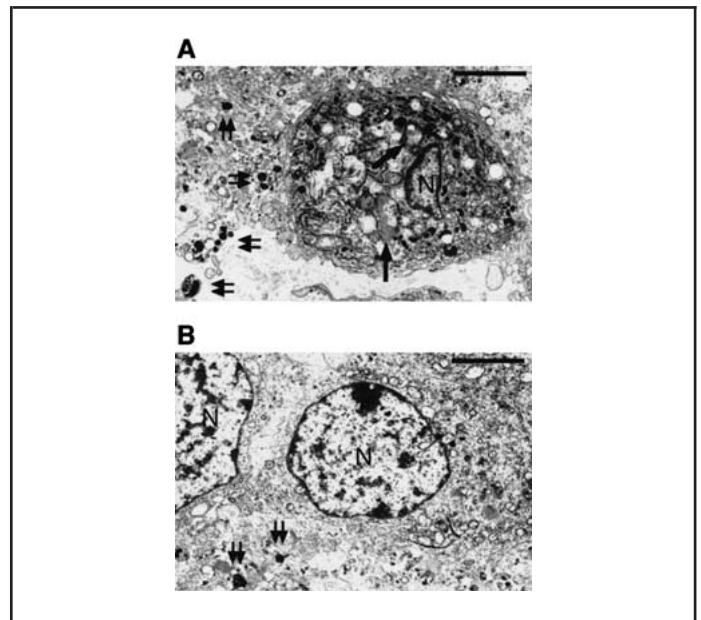
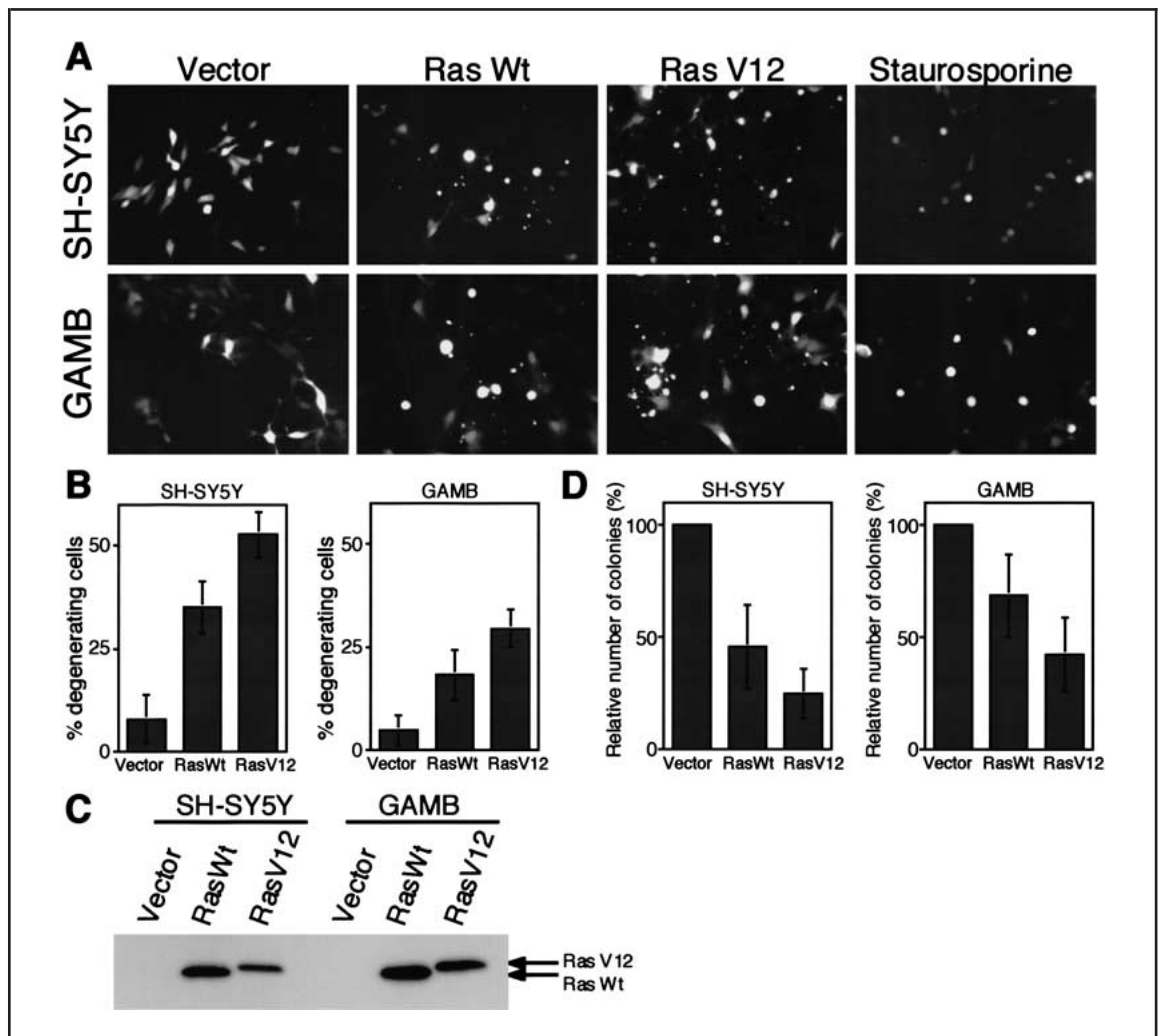


Fig. 2. Transmission electron microscopic analysis of neuroblastoma samples. Degenerating cell (A) and nondegenerating tumor cell (B) found in a neighboring area. The degenerating cell has more electron-dense primary lysosomes (double arrows) as well as secondary lysosomes (single arrows), which are possibly autolysosomes. Degenerating cell is surrounded by cell fragments containing lysosomal structures. N = nucleus. Scale bars = 5 μ m.

shown in Fig. 3, A, when wt-Ras or RasV12 was coexpressed with GFP in SH-SY5Y and GAMB cells, GFP-positive cells showed morphologic degeneration characterized by rounding up and fragmentation into irregular sizes in both cell lines. Cytoplasmic vacuolation was only rarely observed, in contrast to glioma cells, in which Ras induced a cell death characterized by prominent vacuolation (9,16). This morphologic feature of Ras-induced neuroblastoma cell degeneration appeared distinct from that of apoptosis induced by staurosporine treatment or serum deprivation, in which cell fragmentation was not prominent and fragmented cells, if any, were rather of uniform size (Fig. 3, A, and data not shown). Quantitative analysis revealed that, although both wt-Ras and RasV12 induced morphologic degeneration of neuroblastoma cells, RasV12 produced more degenerating cells than wt-Ras (Fig. 3, B). Given that RasV12 is expressed at a level comparable to or lower than wt-Ras (Fig. 3, C), the results indicate that the ability of Ras to induce morphologic degeneration is associated with its activity as an intracellular signaling molecule. We further asked whether the morphologic alteration induced by Ras expression is actually a manifestation of cellular demise. The results of colony formation assays demonstrated that Ras expression suppresses (RasV12 more potently than wt-Ras) clonogenic survival of both neuroblastoma cell lines (Fig. 3, D). Consistent with the idea that the induction of cell death by Ras depends on its activity, RasV12/D38N—having an inactivating point mutation in the Ras effector loop region in a RasV12 background (27)—failed to induce neuroblastoma cell death in either morphologic or colony formation assays (data not shown). These results indicate that Ras expression induces neuroblastoma cell death *in vitro*, most likely through the activation of the downstream signaling pathway(s).

Fig. 3. Induction of neuroblastoma cell death by Ras expression *in vitro*. A–C) Human neuroblastoma cell lines SH-SY5Y and GAMB were cotransfected with 0.5 μ g of the indicated pcDNA3 expression plasmids (Vector, Ras Wt, RasV12) together with the green fluorescent protein (GFP)-expressing plasmid (0.5 μ g). As a control for apoptosis, neuroblastoma cells were transfected with the GFP plasmid alone and treated with staurosporine 24 hours after transfection (Staurosporine). GFP-positive cells were photographed 2 days after transfection or staurosporine treatment (A), and GFP-positive cells showing morphologic degeneration (cells with a rounded or fragmented appearance) were counted as degenerating cells, and a cluster of cell fragments was counted as one degenerating cell) were scored 2 days after transfection. The results are from three separate transfection experiments and are shown in panel (B). Transfected cells were also analyzed for Ras protein expression levels by immunoblotting with anti-H-Ras antibody (C). D) Neuroblastoma cells were transfected with the indicated pcDNA3 expression plasmids (1 μ g), and colony formation assay was done. The results are from three separate transfection experiments. The graph indicates the number of colonies relative to the number of colonies formed by control vector transfection, which was set to 100. In (B) and (D), the error bars represent 95% confidence intervals.



Ras protein expression levels by immunoblotting with anti-H-Ras antibody (C). D) Neuroblastoma cells were transfected with the indicated pcDNA3 expression plasmids (1 μ g), and colony formation assay was done. The results are from three separate transfection experiments. The graph indicates the number of colonies relative to the number of colonies formed by control vector transfection, which was set to 100. In (B) and (D), the error bars represent 95% confidence intervals.

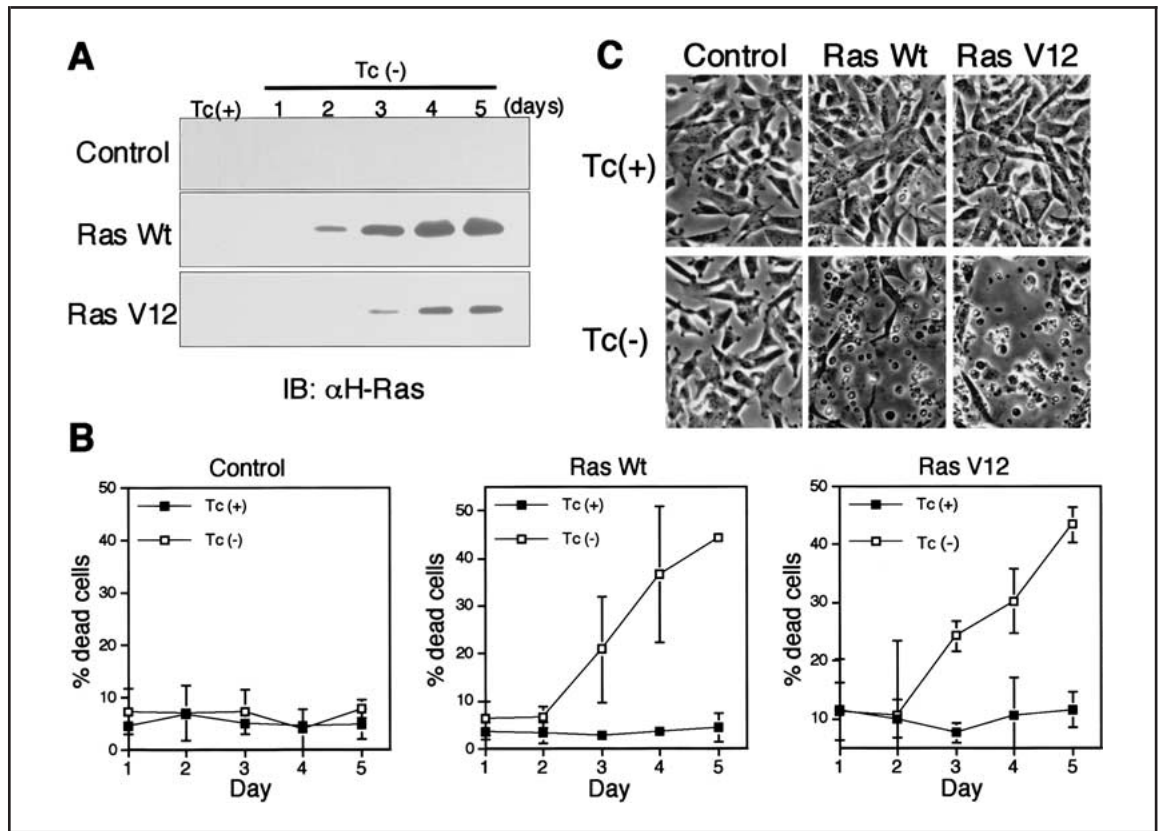
Characterization of Ras-Induced Neuroblastoma Cell Death *In Vitro*

To further characterize Ras-induced neuroblastoma cell death in the absence of secondary effects of transfection, we established stable transfectants of SH-SY5Y cells that can be induced to express wt-Ras or RasV12 following tetracycline withdrawal (Fig. 4, A). Induction of Ras expression increased the proportion of dead cells (Fig. 4, B), and the dying cells were characterized by extensive fragmentation into irregular sizes (Fig. 4, C), as observed in the transient transfection assays (Fig. 3, A). Nuclear staining using propidium iodide revealed that, in contrast to apoptotic cells showing nuclear condensation, fragmented dead cells produced by Ras expression contained nuclear fragments without apparent condensation (Fig. 5, A), which was identical to what occurred *in vivo* in neuroblastoma samples (compare with the fragmented, noncondensed nuclei indicated by double arrows in Fig. 1, D-e). TUNEL analysis indicated that Ras-induced cell death is negative for apoptotic DNA fragmentation (Fig. 5, B). Electron microscopic analysis demonstrated increased lysosomal structures and lack of nuclear changes in cells undergoing Ras-induced death (Fig. 5, C), just as observed

in vivo in tumor samples (Fig. 2). Collectively, these results indicate that Ras expression in neuroblastoma cells triggers nonapoptotic PCD with morphologic features of autophagic degeneration.

We next investigated whether the core regulatory mechanism of apoptotic cell death is involved in Ras-induced nonapoptotic cell death. To this end, we first tested the effect of synthetic (*z*-VAD-fmk and Boc-Asp-fmk) and a viral (p35) pan-caspase inhibitors on Ras-induced neuroblastoma cell death. When the effect of these inhibitors was examined against SH-SY5Y and GAMB cell death caused by transient RasV12 expression, they failed to suppress Ras-induced morphologic degeneration (Fig. 6, A and C) under conditions in which these pan-caspase inhibitors suppressed staurosporine-induced apoptosis (Fig. 6, B and D). Similarly, *z*-VAD-fmk failed to suppress cell death caused by induced expression of wt-Ras in the stable transfectant (Fig. 6, E). We also investigated whether the activation of the caspase cascade, though it may not be essential for cell death induction as shown above, accompanies Ras-induced neuroblastoma cell death. As specific processing of PARP, a common substrate for effector caspases such as caspases-3 and -7, invariably occurs as a result of caspase cascade activation (28), we explored the

Fig. 4. Induction of neuroblastoma cell death *in vitro* by inducible expression of Ras in stable transfectants. **A)** SH-SY5Y-TA-GN (Control), SH-SY5Y-TA-wtRas (Ras Wt), and SH-SY5Y-TA-RasV12 (RasV12) cells cultured in the presence of tetracycline or in its absence for the indicated periods were subjected to immunoblot analysis using anti-H-Ras antibody. **B)** Indicated cells were cultured in the presence and absence of tetracycline, and the percentage of dead cells was determined by the dye exclusion method. The results are from three separate experiments, and the error bars represent 95% confidence intervals. **C)** Phase-contrast micrographs of the indicated cells cultured in presence and absence of tetracycline (Tc[+] and Tc[-], respectively) for 5 days.



evidence of caspase cascade activation in intact cells by immunoblot analysis of PARP. Although PARP was processed to the specific 85-kDa fragment in a pan-caspase inhibitor-inhibitable manner within cells undergoing apoptosis, no such specific

PARP fragment was detected in Ras-expressing cells—even at time points when cell death was evident (Fig. 6, F). We next examined the effect of Bcl-xL expression on Ras-induced neuroblastoma cell death. Bcl-xL is considered to inhibit a wide

Fig. 5. Characterization of neuroblastoma cell death induced by Ras *in vitro*. **(A and B)** Lack of nuclear condensation and apoptotic DNA fragmentation in Ras-induced neuroblastoma cell death. SH-SY5Y-TA-wtRas (Ras Wt) and SH-SY5Y-TA-RasV12 (RasV12) cells cultured in the absence of tetracycline for 5 days as well as parental SH-SY5Y cells either treated with staurosporine or left untreated for 2 days were subjected to propidium iodide staining **(A)** or terminal deoxynucleotidyl transferase-mediated deoxyuridine triphosphate nick-end labeling analysis **(B)**. Phase-contrast micrographs of the corresponding areas are presented in the upper panels. In **(A)**, apoptotic cells are indicated by **arrows**. **C)** Electron micrographs of SH-SY5Y-TA-wtRas cells cultured in the absence (Ras induction [+]) and presence (Ras induction [-]) of tetracycline for 5 days. N = nucleus. Scale bars = 1 μ m.

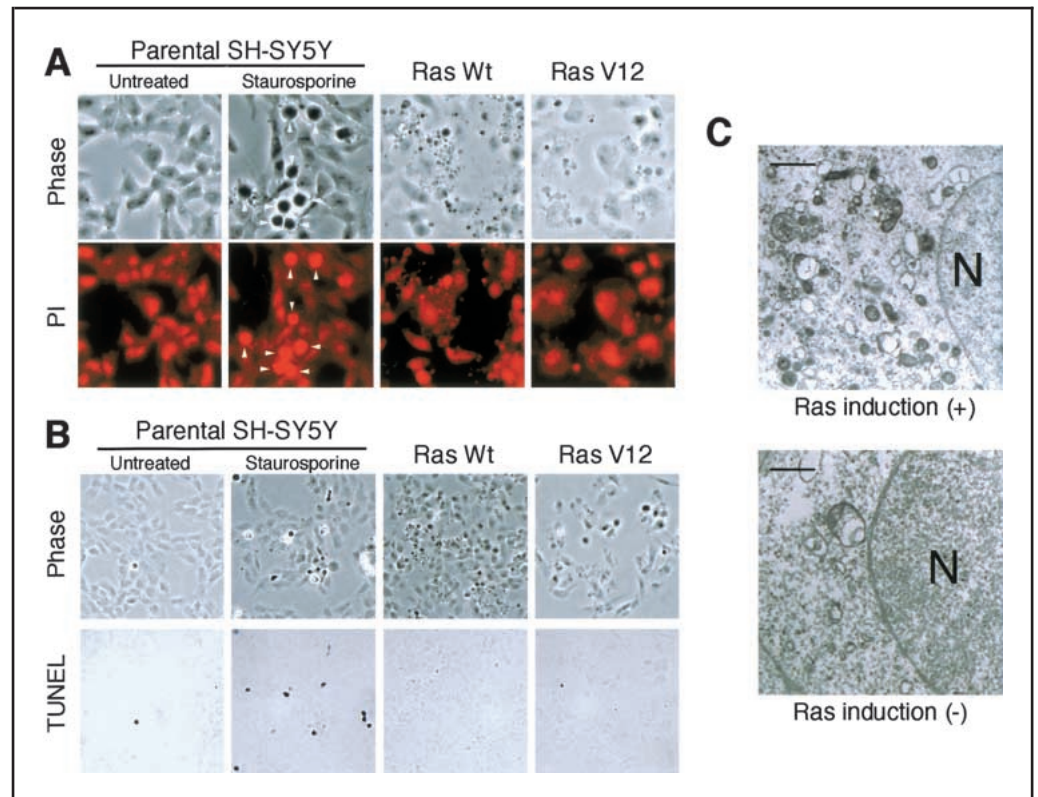
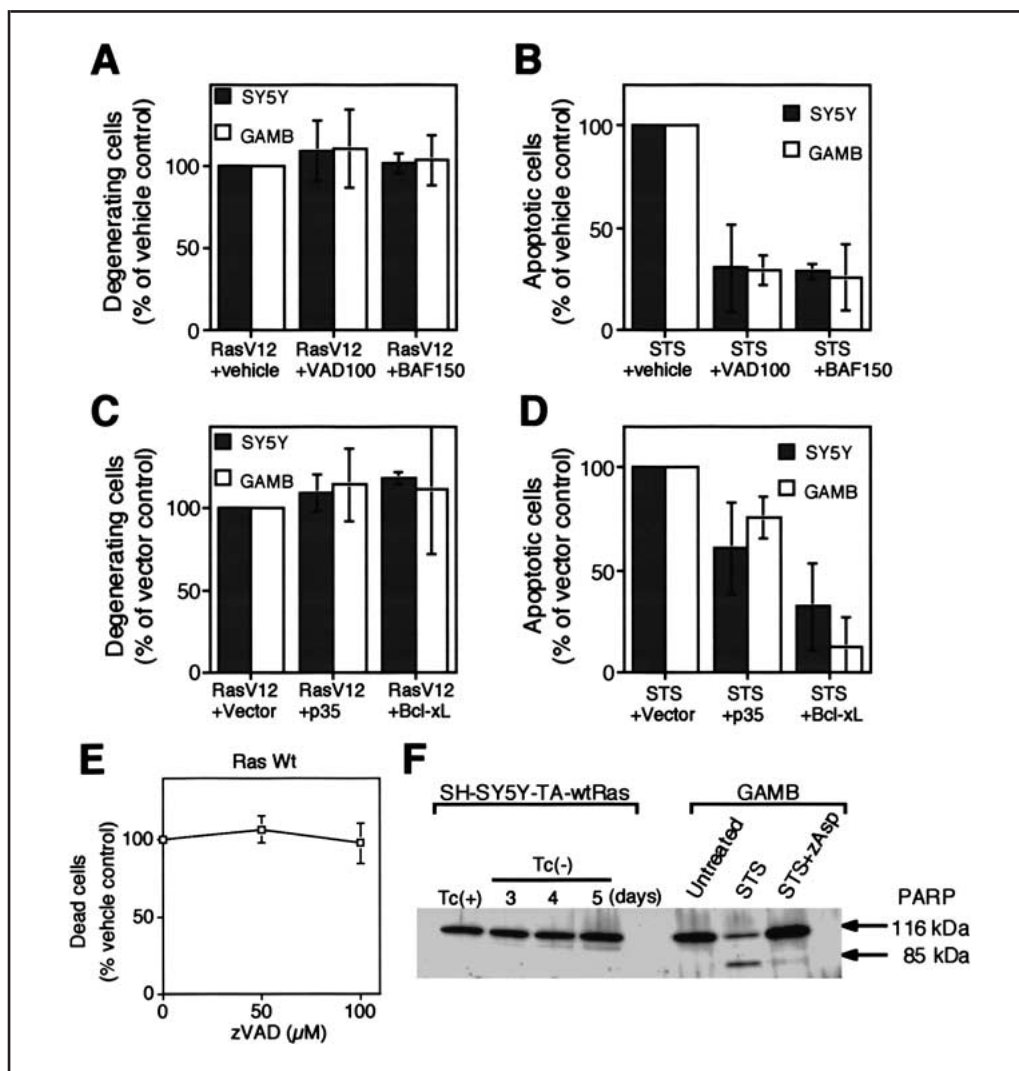


Fig. 6. Lack of role for caspase cascade and Bcl-xL in the regulation of Ras-induced neuroblastoma cell death. **A)** RasV12-expressing pcDNA3 plasmid (0.5 μ g) was cotransfected with the green fluorescent protein (GFP)-expressing plasmid (0.5 μ g) into SH-SY5Y (stippled bars) and GAMB (open bars) neuroblastoma cells in the presence of 100 μ M zVAD-fmk (VAD100) or 150 μ M Boc-Asp-fmk (BAF150) (pan-caspase inhibitors). The proportion of GFP-positive cells showing morphologic degeneration was determined 24 hours after transfection, as described in Fig. 3, B. **B)** SH-SY5Y and GAMB neuroblastoma cells were treated with staurosporine (STS) in the presence of the indicated inhibitors. After 24 hours, cells were stained with acridine orange to detect nuclear changes, and the proportion of apoptotic cells (having condensed and/or fragmented nucleus) was determined under a fluorescence microscope. **C)** SH-SY5Y and GAMB neuroblastoma cells were transfected with the RasV12-expressing pcDNA3 plasmid (0.5 μ g) plus the GFP plasmid (0.5 μ g), together with a control, p35-, or Bcl-xL-expressing plasmid (0.5 μ g). The proportion of GFP-positive cells showing morphologic degeneration was determined 24 hours after transfection, as in (A). **D)** SH-SY5Y and GAMB neuroblastoma cells were transfected with the control pcDNA3 plasmid (0.5 μ g) plus the GFP plasmid (0.5 μ g), together with a control, p35-, or Bcl-xL-expressing plasmid (0.5 μ g). After 24 h, the transfected cells were treated with STS, and the proportion of apoptotic cells was determined by acridine orange staining 24 h after STS treatment as in (B). **E)** SH-SY5Y-TA-wtRas (Ras Wt) cells were cultured in the absence of tetracycline for 5 days in the presence of the indicated concentrations of zVAD-fmk, and the proportion of dead cells was determined by the dye exclusion method. In (A–E), the graphs indicate the percentage of degenerating (A and C), apoptotic (B and D), or dead (E) cells normalized to the vehicle or vector control, and the data represent the means and 95% confidence intervals from three separate experiments. **F)** Cell



lysates were prepared from SH-SY5Y-TA-wtRas cells cultured in the presence or absence of tetracycline for the indicated periods. As a control for caspase-dependent poly(ADP-ribose) polymerase (PARP) processing, cell lysates were prepared from GAMB cells either treated with STS in the presence or absence of the pan-caspase inhibitor zAsp-CH2-DCB (zAsp) or left untreated for 2 days. The cell lysates were subjected to immunoblot analysis using anti-PARP antibody.

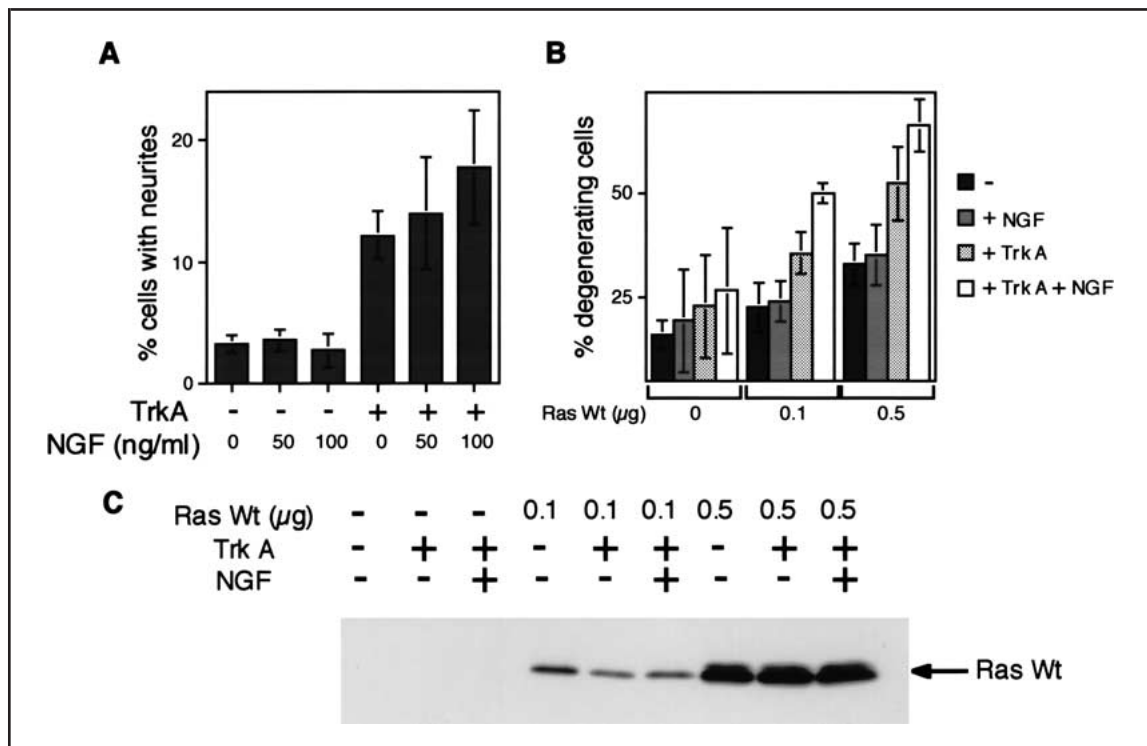
range of both apoptotic and nonapoptotic cell death through maintenance of mitochondrial physiology (29). However, Bcl-xL overexpression failed to inhibit Ras-induced nonapoptotic cell death while efficiently inhibiting staurosporine-induced apoptosis (Fig. 6, C and D). Together, the lack of involvement of caspase cascade and the resistance to Bcl-xL-mediated inhibition indicate that Ras-induced neuroblastoma cell death is regulated by a mechanism essentially distinct from that of apoptosis.

Augmentation of Ras-Induced Neuroblastoma Cell Death by TrkA

Interestingly, coexpression of Ras and TrkA is associated with a better prognosis in neuroblastoma patients than the expression of either alone (12). We hypothesized that TrkA augments the activity of Ras to induce neuroblastoma cell death through its demonstrated ability to activate Ras (30–32), thereby increasing the chance of tumor cell eradication. As reported previously (33), transfection-mediated expression of TrkA (in

the absence of Ras overexpression) induced differentiation of SH-SY5Y cells, and NGF treatment alone failed to induce differentiation but could enhance differentiation induced by TrkA expression (Fig. 7, A). We then assessed the effect of TrkA signaling on Ras-induced neuroblastoma cell death. As shown in Fig. 7, B, the expression of TrkA in the presence of different levels of Ras expression revealed that TrkA expression increases the proportion of degenerating cells in the presence of Ras overexpression much more efficiently than in its absence. Importantly, NGF treatment increased the proportion of degenerating cells in the presence of TrkA expression but not in its absence, providing unequivocal evidence that the augmentation of Ras-induced cell death is mediated by the TrkA signaling pathway. TrkA expression and/or NGF treatment did not affect Ras protein expression itself (Fig. 7, C), indicating that TrkA-mediated augmentation of Ras-induced cell death signaling occurred downstream of Ras expression. These results indicate that TrkA can augment Ras-mediated death signaling, and this synergy of

Fig. 7. Augmentation of Ras-induced neuroblastoma cell death through the activation of the TrkA signaling pathway. **A)** The green fluorescent protein (GFP)-expressing plasmid (0.5 μg) was cotransfected with the TrkA-expressing or the control plasmid (0.5 μg) into SH-SY5Y neuroblastoma cells. The cells were treated 6 hours after transfection with the indicated concentrations of nerve growth factor (NGF) for 1 day, and then GFP-positive cells with neurites (cellular processes longer than two cell-body lengths or longer than one cell-body length with a growth cone) were scored. **B** and **C)** The GFP plasmid (0.5 μg) was cotransfected with the indicated amounts of the wt-Ras-expressing pcDNA3 plasmid with or without the TrkA-expressing plasmid (0.5 μg) into SH-SY5Y cells. The total amount of transfected plasmid DNAs was kept constant by adding empty vector plasmids. The cells were treated 6 h after transfection with or without NGF (100 ng/mL) for 1 day, and then GFP-positive cells showing morphologic degeneration were scored as described in Fig. 3,



TrkA and Ras in neuroblastoma cell death may provide an explanation for the clinical observation that coexpression of TrkA and Ras predicts quite a favorable prognosis (12).

DISCUSSION

Neuroblastoma is quite a heterogeneous clinical entity, ranging from subgroups that have a very favorable prognosis with a high probability of spontaneous regression [such as mass screened neuroblastomas and those assigned to stage 4S according to the INSS (18)] to those that have a very poor prognosis despite aggressive therapies (clinically detected, advanced-stage neuroblastomas, in particular, of patients over 1 year of age) (1,2,10). The molecular basis that distinguishes between neuroblastomas with favorable and poor prognoses is relatively well understood, but the biologic functions of the molecular markers such as H-Ras, TrkA, and N-Myc in neuroblastoma cells have been ill defined. In this study, in an attempt to elucidate the biologic consequence of Ras overexpression in neuroblastoma, we conducted detailed immunohistochemical analyses of neuroblastoma tissues and demonstrated that neuroblastoma cells overexpressing the Ras protein show morphologic changes indicative of cell death. Importantly, degenerating tumor cells positive for Ras did not have morphological features of apoptotic cell death and were essentially negative for TUNEL and active caspase-3 staining, indicating that the mode of cell death is distinct from apoptosis. Of note, although Ras-positive degenerating cells did not show the diffuse, cytosolic staining pattern of active caspase-3 characteristic of apoptosis, they occasionally showed a punctate staining pattern suggestive of the localized caspase-3 activation within autophagic granules (lysosomes) re-

ported by Stadelmann et al. (34) (Kitanaka, C, unpublished observation). In line with such an observation, Ras-positive degenerating cells were often positive for PAS, which can be a marker of autolysosome (23), and ultrastructural analysis of PAS-positive degenerating areas indeed demonstrated autophagic changes of tumor cells, which have been recently described as characteristic degenerative changes in neuroblastoma (8). These immunohistochemical observations together suggested that the overexpression of Ras induces autophagic degeneration of neuroblastoma cells in the absence of caspase cascade activation. To obtain supporting evidence for these *in vivo* observations, we investigated *in vitro*—using neuroblastoma cell lines—whether increased expression of Ras causes such a caspase-independent autophagic degeneration of neuroblastoma cells. The results of *in vitro* analyses indicated that transfection-mediated expression of Ras induces neuroblastoma cell death essentially identical with the tumor cell death observed in neuroblastoma tissues. Ras-induced neuroblastoma cell death was not accompanied by nuclear condensation, apoptotic DNA fragmentation, or caspase cascade activation, but it harbored ultrastructural features of autophagic degeneration. Notably, in contrast to Ras-induced autophagic degeneration of glioma cells characterized by prominent cytoplasmic vacuolation (9,16), Ras-induced neuroblastoma cell degeneration was characterized by cellular fragmentation into irregular sizes and paucity of cytoplasmic vacuolation, in good agreement with the *in vivo* findings obtained from neuroblastoma tissues. Altogether, the precise concordance of *in vivo* and *in vitro* findings strongly supports the idea that increased Ras expression is the cause of caspase-independent autophagic degeneration of neuroblastoma cells observed in tumor samples from neuroblastoma patients.

Our immunohistochemical analyses of neuroblastoma tissues also revealed that focal areas of degeneration overexpressing Ras are occasionally accompanied by “gaps” or “clefts,” suggesting that the degenerating areas are actively shrinking (*see* Fig. 1, C, for example). This implies that Ras-mediated neuroblastoma cell degeneration can contribute, at least locally, to volume reduction (regression) of tumor. We therefore asked whether such a local mechanism of regression is indeed associated with overall regression of neuroblastoma. Among subgroups of neuroblastomas, at least one third of mass screened neuroblastomas have been reported to undergo spontaneous regression (2,17), while clinically detected, advanced-stage neuroblastomas from patients over 1 year of age are presumed to have a very low chance of regression. The immunohistochemical analysis of tumor samples from these subgroups of neuroblastoma indicated that degenerating tumor cells overexpressing Ras are found much more frequently in mass screened neuroblastomas than in clinically detected, advanced-stage neuroblastomas from patients over 1 year of age, establishing a clear correlation between Ras-associated degeneration and the propensity to undergo spontaneous regression. Although it may not necessarily exclude the existence of other mechanisms, this clear correlation strongly supports the idea that Ras-mediated nonapoptotic tumor cell death plays an important role in spontaneous regression of neuroblastoma. This idea explains why previous observations failed to establish a definite correlation between apoptosis and factors associated with spontaneous regression (5–7), and our results thus provide a novel and significant insight into the mechanism underlying spontaneous neuroblastoma regression. It may also be extrapolated that, even in neuroblastomas unlikely to regress spontaneously, Ras expression contributes to a favorable prognosis by facilitating nonapoptotic tumor cell death in conjunction with anticancer treatments. In support of this idea, recent observations indicate that autophagic changes are prominent not only in untreated but also in treated neuroblastomas (8) and that an anticancer drug (fenretinide) can induce nonapoptotic cell death in neuroblastoma cell lines in a caspase-independent manner (35). While our results thus suggest that increased Ras expression likely contributes to a favorable prognosis through induction of nonapoptotic tumor cell death, it is also possible that Ras does so through other mechanisms. Indeed, we observed modest H-Ras immunoreactivity in tumor cells showing ganglionic maturation in some cases (Kato, K, unpublished observation). It would therefore be interesting to speculate that Ras negatively regulates the growth of neuroblastoma by inducing cell death when expressed at higher levels and differentiation when expressed at lower levels.

At present, it remains unknown what triggers Ras expression in neuroblastoma. Our observations that Ras-positive cells are located both distant from and close to fibrovascular stroma suggest that it is unlikely to be local environmental factors, including ischemic conditions. Rather, inherent genetic control seems more plausible. Presumably, in neuroblastomas that ultimately regress, tumor cells are programmed to express Ras, and the proportion of Ras-overexpressing tumor cell subpopulations may be increasing during the regression phase, though it would not be ethically acceptable to obtain surgical specimens from actively regressing neuroblastomas to examine this. In neuroblastomas that do not ultimately regress, however, tumor cell subpopulations that are programmed to express Ras may undergo local regression within the tumor; but they will eventually

be outgrown by other subpopulations that are not programmed to express Ras. The molecular mechanism by which Ras protein expression is regulated in neuroblastoma also remains unknown, but the mechanism appears to be either transcriptional or post-transcriptional, as H-Ras overexpression in neuroblastoma is not accompanied by H-ras gene amplification (11). In this respect, it would be interesting to note that the expression of N-Myc, a well-established predictor of a poor prognosis of neuroblastoma (10), is inversely correlated with H-Ras expression in neuroblastomas (14). It is, therefore, possible that N-Myc may contribute to poor prognosis through inhibition of H-Ras expression. At any rate, elucidation of the molecular mechanism involved in the regulation of Ras expression may enable us to artificially manipulate Ras expression in neuroblastomas and thus open a novel avenue to neuroblastoma therapy.

Finally, this study for the first time to our knowledge reveals the role of caspase cascade-independent, nonapoptotic cell death in human diseases or healthy conditions. Nonapoptotic PCD now appears to be involved in more diverse *in vivo* processes than has been previously assumed (9,36). In this sense, this study sets the first good example that exploration of the roles and mechanisms of nonapoptotic PCD under physiological and pathological conditions could bring about important progress in biomedical science that would not be possible by apoptosis research alone. Our study also indicates for the first time the significance of caspase cascade-independent, nonapoptotic PCD in the growth control of cancer. Elucidation of the molecular mechanisms of nonapoptotic PCD is expected to contribute to the development of novel therapeutic strategies against human diseases, including cancer, which often acquires resistance against apoptotic cell death during development (37).

REFERENCES

- (1) Pritchard J, Hickman JA. Why does stage 4s neuroblastoma regress spontaneously? *Lancet* 1994;344:869–70.
- (2) Yamamoto K, Hanada R, Kikuchi A, Ichikawa M, Aihara T, Oguma E, et al. Spontaneous regression of localized neuroblastoma detected by mass screening. *J Clin Oncol* 1998;16:1265–9.
- (3) Oue T, Fukuzawa M, Kusafuka T, Kohmoto Y, Imura K, Nagahara S, et al. In situ detection of DNA fragmentation and expression of *bcl-2* in human neuroblastoma: relation to apoptosis and spontaneous regression. *J Pediatr Surg* 1996;31:251–7.
- (4) Hoehner JC, Gestblom C, Olsen L, Pahlman S. Spatial association of apoptosis-related gene expression and cellular death in clinical neuroblastoma. *Br J Cancer* 1997;75:1185–94.
- (5) Koizumi H, Wakisaka M, Nakada K, Takakuwa T, Fujioka T, Yamate N, et al. Demonstration of apoptosis in neuroblastoma and its relationship to tumour regression. *Virchows Arch* 1995;427:167–73.
- (6) Ikeda H, Hirato J, Akami M, Matsuyama S, Suzuki N, Takahashi A, et al. Bcl-2 oncoprotein expression and apoptosis in neuroblastoma. *J Pediatr Surg* 1995;30:805–8.
- (7) Tonini GP, Mazzocco K, di Vinci A, Geido E, de Bernardi B, Giaretti W. Evidence of apoptosis in neuroblastoma at onset and relapse. An analysis of a large series of tumors. *J Neurooncol* 1997;31:209–15.
- (8) Kodet R. Ultrastructural observations on neuroblastic tumors in childhood: a study of tumor cell differentiation and regression on 89 cases. *Cesk Patol* 1998;34:123–30.
- (9) Kitanaka C, Kuchino Y. Caspase-independent programmed cell death with necrotic morphology. *Cell Death Differ* 1999;6:508–15.
- (10) Brodeur GM. Molecular basis for heterogeneity in human neuroblastomas. *Eur J Cancer* 1995;31A:505–10.
- (11) Tanaka T, Slamon DJ, Shimada H, Shimoda H, Fujisawa T, Ida N, et al. A significant association of Ha-ras p21 in neuroblastoma cells with patient prognosis. A retrospective study of 103 cases. *Cancer* 1991;68:1296–302.

- (12) Tanaka T, Sugimoto T, Sawada T. Prognostic discrimination among neuroblastomas according to Ha-*ras/trk A* gene expression: a comparison of the profiles of neuroblastomas detected clinically and those detected through mass screening. *Cancer* 1998;83:1626–33.
- (13) Matsunaga T, Takahashi H, Ohnuma N, Tanabe M, Yoshida H, Iwai J, et al. Expression of *N-myc* and *c-src* protooncogenes correlating to the undifferentiated phenotype and prognosis of primary neuroblastomas. *Cancer Res* 1991;51:3148–52.
- (14) Nakada K, Fujioka T, Kitagawa H, Takakuwa T, Yamate N. Expressions of *N-myc* and *ras* oncogene products in neuroblastoma and their correlations with prognosis. *Jpn J Clin Oncol* 1993;23:149–55.
- (15) Nakagawara A, Arima-Nakagawara M, Scavarda NJ, Azar CG, Cantor AB, Brodeur GM. Association between high levels of expression of the TRK gene and favorable outcome in human neuroblastoma. *N Engl J Med* 1993;328:847–54.
- (16) Chi S, Kitanaka C, Noguchi K, Mochizuki T, Nagashima Y, Shirouzu M, et al. Oncogenic Ras triggers cell suicide through the activation of a caspase-independent cell death program in human cancer cells. *Oncogene* 1999;18:2281–90.
- (17) Nishihira H, Toyoda Y, Tanaka Y, Ijiri R, Aida N, Takeuchi M, et al. Natural course of neuroblastoma detected by mass screening: a 5-year prospective study at a single institution. *J Clin Oncol* 2000;18:3012–7.
- (18) Brodeur GM, Pritchard J, Berthold F, Carlsen NL, Castel V, Castleberry RP, et al. Revisions of the international criteria for neuroblastoma diagnosis, staging, and response to treatment. *J Clin Oncol* 1993;11:1466–77.
- (19) Furth ME, Aldrich TH, Cordon-Cardo C. Expression of *ras* proto-oncogene proteins in normal human tissues. *Oncogene* 1987;1:47–58.
- (20) Kouroku Y, Urase K, Fujita E, Isahara K, Ohsawa Y, Uchiyama Y, et al. Detection of activated Caspase-3 by a cleavage site-directed antiserum during naturally occurring DRG neurons apoptosis. *Biochem Biophys Res Commun* 1998;247:780–4.
- (21) Ijiri R, Tanaka Y, Kato K, Misugi K, Nishihira H, Toyoda Y, et al. Clinicopathologic study of mass-screened neuroblastoma with special emphasis on untreated observed cases: a possible histologic clue to tumor regression. *Am J Surg Pathol* 2000;24:807–15.
- (22) Hiyama E, Hiyama K, Ohtsu K, Yamaoka H, Ichikawa T, Shay JW, et al. Telomerase activity in neuroblastoma: is it a prognostic indicator of clinical behaviour? *Eur J Cancer* 1997;33:1932–6.
- (23) Geddes JF, Thom M, Robinson SF, Revesz T. Granular cell change in astrocytic tumors. *Am J Surg Pathol* 1996;20:55–63.
- (24) Bennett SA, Stevenson B, Staines WA, Roberts DC. Periodic acid-Schiff (PAS)-positive deposits in brain following kainic acid-induced seizures: relationships to *fos* induction, neuronal necrosis, reactive gliosis, and blood-brain barrier breakdown. *Acta Neuropathol (Berl)* 1995;89:126–38.
- (25) Ballas K, Lyons J, Janssen JW, Bartram CR. Incidence of *ras* gene mutations in neuroblastoma. *Eur J Pediatr* 1988;147:313–4.
- (26) Moley JF, Brother MB, Wells SA, Spengler BA, Biedler JL, Brodeur GM. Low frequency of *ras* gene mutations in neuroblastomas, pheochromocytomas, and medullary thyroid cancers. *Cancer Res* 1991;51:1596–9.
- (27) Abdellatif M, Schneider MD. An effector-like function of Ras GTPase-activating protein predominates in cardiac muscle cells. *J Biol Chem* 1997;272:525–33.
- (28) Nicholson DW. Caspase structure, proteolytic substrates, and function during apoptotic cell death. *Cell Death Differ* 1999;6:1028–42.
- (29) Green DR, Reed JC. Mitochondria and apoptosis. *Science* 1998;281:1309–12.
- (30) Li BQ, Kaplan D, Kung HF, Kamata T. Nerve growth factor stimulation of the Ras-guanine nucleotide exchange factor and GAP activities. *Science* 1992;256:1456–9.
- (31) Burchill SA, Berry PA, Lewis IJ. Activation of p21ras by nerve growth factor in neuroblastoma cells. *J Neurol Sci* 1995;133:3–10.
- (32) Segal RA, Greenberg ME. Intracellular signaling pathways activated by neurotrophic factors. *Annu Rev Neurosci* 1996;19:463–89.
- (33) Lavenius E, Gestblom C, Johansson I, Nanberg E, Pahlman S. Transfection of *TRK-A* into human neuroblastoma cells restores their ability to differentiate in response to nerve growth factor. *Cell Growth Differ* 1995;6:727–36.
- (34) Stadelmann C, Deckwerth TL, Srinivasan A, Bancher C, Bruck W, Jellinger K, et al. Activation of caspase-3 in single neurons and autophagic granules of granulovacuolar degeneration in Alzheimer's disease. Evidence for apoptotic cell death. *Am J Pathol* 1999;155:1459–66.
- (35) Maurer BJ, Metelitsa LS, Seeger RC, Cabot MC, Reynolds CP. Increase of ceramide and induction of mixed apoptosis/necrosis by *N*-(4-hydroxyphenyl)-retinamide in neuroblastoma cell lines. *J Natl Cancer Inst* 1999;91:1138–46.
- (36) Chautan M, Chazal G, Cecconi F, Gruss P, Golstein P. Interdigital cell death can occur through a necrotic and caspase-independent pathway. *Curr Biol* 1999;9:967–70.
- (37) Evan GI, Vousden KH. Proliferation, cell cycle and apoptosis in cancer. *Nature* 2001;411:342–8.

NOTES

We are grateful to Tomo Yasuda for excellent technical assistance and to Kumiko Todate for generous secretarial assistance. This work was supported by a Grant-in-Aid from the Ministry of Health, Labour and Welfare of Japan for the second-term Comprehensive 10-Year Strategy for Cancer Control (Y. Kuchino) and by grants from the Ministry of Health, Labour and Welfare of Japan (Y. Kuchino) and from the Ministry of Education, Culture, Sports, Science and Technology of Japan for cancer research (C. Kitanaka and Y. Kuchino).

Manuscript received August 23, 2001; revised November 21, 2001; accepted January 22, 2002.